Wheat canopy structure and surface roughness effects on multiangle observations at L-Band

S. Peischl, J.P. Walker, D. Ryu, Yann H. Kerr, R. Panciera, C. Rüdiger

Wheat canopy structure and surface roughness effects on multi-angle observations at L-band

Journal:	*Transactions on Geoscience and Remote Sensing*
Manuscript ID:	Draft
Manuscript Type:	Soil Moisture and Ocean Salinity Mission 2010 Special Issue paper
Keywords:	Remote sensing, Microwave radiometry

Wheat canopy structure and surface roughness effects on multi-angle observations at L-band

Sandy Peischl, *Member, IEEE,* Jeffrey P. Walker, Dongryeol Ryu, *Member, IEEE*, Yann Kerr, *Senior Member, IEEE,* Rocco Panciera, Christoph Rüdiger, *Member, IEEE*

Contact details:

Sandy Peischl

Department of Civil Engineering

Building 60, Room 156, Clayton

Monash University Victoria 3800

Australia

Phone: +61 3 990 54957

Fax: +61 3 990 54944

E-mail: sandy.peischl@monash.edu

***Abstract*—**The capability of multi-angle observations of the Soil moisture and Ocean Salinity (SMOS) mission is expected to significantly improve the inversion of soil microwave emissions for soil moisture by enabling the simultaneous retrieval of the vegetation optical depth and other surface parameters. Consequently, this paper investigates the relationship between soil moisture and brightness temperature at multiple incidence angles using airborne L-band data from the National Airborne Field Experiment (NAFE) in Australia in 2005. A forward radio brightness model was used to predict the passive microwave response at a range of incidence angles, given inputs of i) ground measured soil and vegetation properties and ii) default model parameters for vegetation and roughness characterization. Simulations were made across various dates and locations with wheat cover and evaluated against the available airborne observations. The comparison showed a significant underestimation of the measured brightness temperatures by the model, when using the default parameterization. This discrepancy subsequently led to a soil moisture retrieval error of up to 0.3 m^3m^{-3}. The analysis found that i) the roughness value H_r was too low, which was then adjusted as a function of the soil moisture; while ii) the vegetation structure parameters tt_h and tt_v were reduced by calibrating them from a single flight and testing them for different moisture conditions and locations. The simulation error between the forward model predictions and the airborne observations was improved from rmse=31.3 K (26.5 K) to rmse=2.3 K (5.3 K) for wet and (dry) soil moisture conditions, respectively.

Index Terms—L-band Microwave Emission of the Biosphere (L-MEB), National Airborne Field Experiment (NAFE), Microwave radiometry, Multi-angle, Remote Sensing, Soil Moisture and Ocean Salinity (SMOS)

I. INTRODUCTION

The potential of passive microwave systems to monitor surface soil moisture has been extensively studied during the past decades [1]-[7] and are considered as one of the most relevant techniques. Microwave remote sensing is in particular suitable due to i) its high sensitivity to the dielectric properties of the soil-water medium, which can be directly related to the water content, ii) the reduced interference with the atmosphere and surface roughness, iii) the low attenuation effects of the vegetation layer and iv) its all-weather capability. Moreover, at low frequencies the penetration depth within the soil column is significant compared to other wavelengths. Hence, especially the protected L-band (~1-2 GHz) with a penetration depth of typically ~5 cm and low sensitivity to canopy and surface roughness is preferred for the purpose of soil moisture remote sensing. Consequently, the strong scientific demand for large scale L-band observations of soil moisture data, with a sufficient temporal resolution for application in hydrological, meteorological and agronomical disciplines [8], led to the first spaceborne mission specifically dedicated to the monitoring of soil moisture.

The Soil Moisture and Ocean Salinity (SMOS) satellite was launched in November 2009 by the European Space Agency (ESA) and designed to provide global maps of the surface soil moisture fields with an accuracy better than 0.04 m^3m^{-3} for the nominal case of bare or low vegetated soils (non-nominal cases include mountainous and urban areas, frozen or very dry soils, ice and significant snow covered surfaces) [9],[10]. Importantly, the satellite's new antenna concept utilizes a 2-dimensional interferometric L-band radiometer to overcome the constraints given by the proportional relation between the antenna diameter and the resulting spatial resolution and hence achieves the desired pixel size of less than 50 km. Moreover one of the innovative features of SMOS is its capability of multi-incidence angle observations, that are obtained by the along-track movement of the satellite and the corresponding quasi-simultaneous acquisition of a series of brightness temperatures for a range of angles over the same location on earth. Previous studies [11]-[13] have shown that there are significant angular signatures on the measured radiometer signal associated with various land surface features and that in some cases it is difficult to separate the contribution of the vegetation from the actual soil emission based on single angle measurements. Thus, by understanding these angular dependencies, it has been suggested that model parameters such as vegetation attenuation and surface roughness may be simultaneously estimated, resulting in an enhanced and presumably more accurate soil moisture retrieval [14]. Due to the absence of comparable spaceborne observations regarding the novel SMOS configuration, retrieval algorithms such as L-MEB (L-band and Microwave Emission of the Biosphere [15]) have been primarily tested and developed using synthetic simulations [16] and small scale field experiments (SMOSREX [17], MELBEX [18] and EuroSTARRS [19]), with the modeling of incidence angle relationships based on only a subset of the possible land cover types. Consequently, the derived relationships and the model interactions between land surface variables and observed brightness temperature response need to be verified at larger spatial scales and extended for a wider range of land surface conditions.

The objective of this paper is to compare multi-angle L-band data from airborne observations with simulated brightness temperatures using the L-MEB model and ground truth data as input. Subsequently, the performance of the forward model parameterization is evaluated based on different soil moisture conditions and locations and additional parameterizations are tested, that included i) modifications of the modeled roughness and vegetation structure characterization.

II. Experimental data set

The multi-incidence angle airborne data used in this paper were acquired in November 2005 during the National Airborne Field Experiment (NAFE'05) in south-east Australia. The campaign was conducted over a period of four weeks including a combination of airborne observations and ground measurements. A complete description of the experiment and the data collection strategy is provided in [20], so only the pertinent details are summarized here.

A. Study Area

The field experiment concentrated on the northern part of the Goulburn River catchment (32° S, 150° E) located in New South Wales, Australia. The 40 km × 40 km study region had been subdivided into two main focus areas within the Merriwa River and Krui River catchment. Across each of these two focus areas several smaller sites had been selected for intensive airborne and ground operations at farm-scale. The multi-incidence angle flights, which are the emphasis of this study, covered only three out of a total of eight focus farms including Midlothian, Merriwa Park and Cullingral (Fig. 1). The observed terrain is fairly flat, with soil types ranging from clay loams to sandy soils [21]. The regional climate can be described as sub-humid and temperate with an average annual rainfall of 700 mm and a mean maximum annual temperature of 30°C in summer and 16°C in winter. During the campaign period the focus farms were dominated by grazing lands with native grass cover and cropping land use (mainly wheat, barley and lucerne).

B. Airborne multi-angle Data

The primary airborne instrument used in the NAFE'05 campaign was the Polarimetric L-band Multi-beam Radiometer (PLMR), which operates at a frequency of 1.413 GHz with a bandwidth of 24 MHz. During the field experiment the L-band radiometer was typically used to measure dual-polarized brightness temperatures in pushbroom mode at six viewing angles (±7°, ±21.5°, ±37.5°). However, regarding the multi-angle data collection, PLMR was mounted on the aircraft in an along-track configuration, resulting in three PLMR beams pointing forward and three backward with respect to the flight direction of the aircraft. Consequently, as the aircraft moved along its flight path, this setup provided a minimum of six quasi-simultaneous multi-incidence angle observations of the same location on earth with a 17° (3-dB) antenna beamwidth. The nominal flight altitude was about 750 m which corresponds to a spatial resolution of approximately 250 m. In general, an area of 1.5 km × 6 km was covered by four to five parallel South-North oriented flight lines at each of the three farms. Dual-polarized multi-angle data were acquired on four days (once a week) at Merriwa Park, and one day each for Midlothian and Cullingral, respectively. Additionally, specific dive flights (i.e. successive steep ascents/descents) were conducted immediately following the multi-angle flights over the focus farms in order to provide observations with an even wider range of incidence angles (~3-60°).

Calibration of the PLMR instrument was carried out on a daily basis before and after the flight using both the sky (cold calibration) and a blackbody box (warm calibration) as target. Supplementary in-flight calibration checks were made through flights over a large water body that was continuously monitored in terms of surface water temperature and salinity. A detailed description of the complete calibration procedures can be found in [20]. Considering the range of brightness temperature measurements over land during the campaign (150-300 K), the PLMR accuracy was estimated by [20] to be higher than 0.7 K for H-polarization and 2 K for V-polarization. The calibrated radiometer observations have further been processed to provide local incidence angle and effective footprint size information taking into account ground topography, aircraft position and attitude. Finally, the data were filtered to eliminate large aircraft yaw and roll angles due to turbulences and wind forces. As a result, sun glint effects in the external beams were also reduced.

C. Ground Data

Extensive ground sampling activities were conducted coincident with the airborne observations, focusing on an area of approximately 1.5 km × 3.0 km at each farm (see Fig. 1). The measurements of near-surface soil moisture (0-5 cm) were made using the Hydraprobe Data Acquisition System (HDAS, [22]), which consists of a Hydraprobe soil moisture sensor, a Global Positioning System (GPS) and a handheld pocket PC that has a Geographic Information System (GIS) installed to provide a visual output of the sampling location and the corresponding soil moisture observation. The HDAS measurements were made over a spatial sampling grid with varying spacing from 6.25 m to 2 km. The high-resolution sampling (6.25 m - 12.5 m) was mainly concentrated on an area of 150 m × 150 m within the cropping fields at Merriwa Park and Cullingral and within a large patch of native grass at Midlothian. The surrounding areas were sampled at coarser spatial scales. The Hydraprobe standard soil moisture product was calibrated against gravimetric soil samples from the field and laboratory data and corrected for temperature effects, resulting in an estimated accuracy of ±0.033 m^3m^{-3} [22]. The gravimetric samples were further analyzed in terms of soil texture and soil properties (Table I). Supplementary data including land use, surface roughness, rock cover fraction, rock temperature, dew amount, vegetation biomass and vegetation water content were also recorded at each farm site. Climate data were available through an existing in-situ monitoring network (www.eng.newcastle.edu.au/sasmas/SASMAS/sasmas.htm) collecting long-term soil moisture (0-5 cm, 0-30 cm, 30-60 cm and 60-90 cm), soil temperature (0-5 cm and 0-30 cm) and rainfall data. During the campaign a few stations were temporarily upgraded with additional instrumentation including thermal infrared sensors (TIR), surface soil-temperature profiles (1 cm, 2.5 cm and 4 cm) and leaf wetness sensors to determine the presence of dew. Midlothian, Merriwa Park and Cullingral were each equipped with one permanent and one temporary monitoring station. The latter was always located within the high-resolution soil moisture sampling area of the focus farm.

This paper focuses on the use of multi-incidence angle airborne observations and ground data collected across the cropping fields at Merriwa Park and Cullingral. Both sites were covered by mature wheat, whereas Midlothian was predominantly characterized by native grass and lucerne. Consequently, data collected across the Midlothian site was not considered in this study. Table I summarizes the main features of the Merriwa Park and Cullingral study sites showing an overall dynamic soil moisture range of about 0.05-0.55 m^3m^{-3} for Merriwa Park over the entire period. Moist soil conditions were generally observed at the start of the campaign in response to significant rainfall in the area, while towards the end of the field experiment the topsoil showed substantial drying effects. Cullingral was only covered once with multi-angle flights and corresponding in-situ soil moisture measurements during the campaign. The spatial soil moisture distribution across Cullingral ranged from 0.05-0.25 m^3m^{-3} on the observation day.

III. Radiative transfer model

The radiative transfer model used in this study is the L-band Microwave Emission of the Biosphere (L-MEB) model [15], which is the core element of the operational soil moisture retrieval algorithm developed for SMOS [23]. A detailed description of the model structure and parameterization is presented in [15], so the following discussion concentrates only on the basic principles of L-MEB.

The presence of vegetation and the resulting interaction with the soil surface emission are described in terms of a simplified (zero-order) solution of the radiative transfer approach, also known as the tau-omega model. This algorithm assumes that the influence of the vegetation layer on the *p*-polarized soil reflectivity (r_{GP}) is accounted for by vegetation attenuation (Υ_P) and scattering effects (ω) and results in a composite brightness temperature (TB_P) as follows:

$$TB_P = (1-\omega_P)(1-\Upsilon_P)(1+\Upsilon_P r_{GP})T_C + (1-r_{GP})\Upsilon_P T_G, \tag{1}$$

where T_G and T_C correspond to the effective soil and vegetation temperature [K], respectively. The reflectivity of the underlying soil surface (r_{GP}) is a function of the wave polarization, the observation frequency and the incidence angle, and can be quantified for non-smooth surfaces by calculating the smooth surface Fresnel reflectivity (r_{GP}*) and adjusting it through the use of a set of soil roughness parameters (i.e. H_r and N_{rp}):

$$r_{GP} = r_{GP}{*} \cdot \exp\left[-H_R \cos(\theta)^{N_{RP}}\right]. \tag{2}$$

Note, that N_{rp} is introduced to parameterize the angular dependence of the surface roughness. The attenuation effect caused by the canopy, also referred to as transmissivity, is expressed as a function of the vegetation optical depth (τ_P) and the incidence angle (θ):

$$\Upsilon_p = \exp\left(-\tau_P / \cos(\theta)\right). \tag{3}$$

The optical depth in turn can be computed as a linear function of the vegetation water content (*VWC*) and the empirical parameter b_p, which is mainly dependent on the sensor frequency, polarization, canopy type and plant structure [24]:

$$\tau_{nad} = VWC \cdot b_p \ . \tag{4}$$

Since (4) is strictly valid for nadir observations (θ=0°), two additional specific vegetation structure parameters tt_h, tt_v (h and v denoting horizontal and vertical polarization) are introduced that account for the angular effect on the optical depth and hence on the vegetation transmissivity:

$$\tau_p = \tau_{nad} (\sin^2(\theta) \cdot tt_p + \cos^2(\theta)) \ . \tag{5}$$

Considering a value of tt_P>1 or tt_P<1 results either in an increasing or decreasing trend of the optical depth, respectively, as a function of the incidence angle. The particular case of tt_v=tt_h=1 corresponds to the isotropic state, where the optical depth of the standing canopy is assumed to be independent of both polarization and incidence angle.

IV. MODELING APPROACH AND PARAMETERIZATION

The L-MEB forward model was used to generate dual-polarized brightness temperatures at a range of incidence angles and moisture conditions by implementing the NAFE'05 data described in Section II. The model set up was based on two types of input parameters: i) default model parameters as a function of the land cover class and ii) ground truth information collected at the focus farms. The available ground data for the two focus farms Merriwa Park and Cullingral included soil moisture, soil texture, bulk density, soil profile temperature, vegetation water content and vegetation temperature data. The input soil moisture was calculated by averaging all high-resolution, near-surface ground measurements falling within the same PLMR footprint for each observation day. The total number of HDAS measurements was generally between ~250-300 points per observation day and radiometer footprint. Further model input included a special set of parameters for surface roughness and vegetation characterization, i.e. variables H_R and N_{RP} for the soil layer and tt_P, ω_p and b_P for the wheat canopy. These values were sourced from the study by [15], in which the parameters had been calibrated from the PORTOS-93 experiment over wheat at the Avignon test site in France [25]. This parameterization proposed by [15] is hereafter referred to as the 'default' parameter set. Using the ground data and the default parameterization, brightness temperature estimates were calculated for both H- and V-polarization and incidence angles ranging from 0-50°. The forward simulations were done for all available dates at Merriwa Park and Cullingral with the L-MEB results compared against the actual airborne multi-incidence angle observations of the corresponding day and test site. Further to the default model simulations described above, two additional parameter sets were tested based on modifications of the initial model parameterization (Table II). In the second forward model approach the default parameterization was changed in terms of a single model parameter; the soil roughness value H_R given in [15] was replaced by a soil moisture dependent roughness value proposed by [26] for the same study site. The basis for using a soil roughness value as a function of soil moisture is due to a phenomenon known as "dielectric roughness", which contributes to volume scattering of the signal coming from deeper soil layers, and is assumed to be caused by a variation of dielectric properties within the soil column due to a non-uniform distribution of the water particles at micro-scale [27],[28]. Thus, in addition to the spatial variations in the surface height ("geometric roughness"), it has been postulated that the "dielectric roughness" should also be accounted for in terms of an effective H_R parameter. The study by [26] was based on high-resolution (62.5 m), single-angle PLMR data from the NAFE'05 experiment and suggested that the default H_R value in L-MEB was too low for vegetation with dominant vertical structure such as wheat and barley. Note that [29] also had to increase the H_R parameter for their studies when they used airborne L-band data over the same test site but acquired by the EMIRAD radiometer, suggesting that the higher roughness values were not related to an instrument-specific bias of the PLMR instrument itself. Moreover, [26] found that the on-site calibrated H_R value demonstrated a notable temporal variation which correlated with the observed moisture conditions during the field experiment. These results were consistent with those published by [30] over bare soil at the SMOSREX test site. Hence [26] developed a simple linear relationship between H_R and the soil moisture content for the NAFE'05 test sites, which estimated lower H_R values with increasing moisture content. Considering these results, the second parameterization had been set to include a roughness value specifically calculated for each observation date depending on the corresponding soil moisture information of that day. Note that since this linear function is soil type-specific, the defined relationship between roughness effects and soil moisture is different for Merriwa Park and Cullingral, where the soil texture changes from silty clay loam to silty loam, respectively (see Table I).

The third parameter set included two modifications compared to the default L-MEB parameterization: i) H_R calculated as a function of the actual soil moisture content (as in the second model approach) and ii) calibrated vegetation structure variables tt_h and tt_v using the available multi-incidence data for one of the four observation days. These vegetation parameters were estimated through an optimization routine which had been applied to a single flight day

272 over Merriwa Park (9 November 2005). The calibrated values for tt_h and tt_v corresponded, respectively, to a decrease (tt_h <1) and increase (tt_v >1) of the optical depth with the incidence angle at each polarization, which was expected due to the dominantly vertical structure of the wheat canopy. This parameterization was then applied to all remaining observation days at Merriwa Park to assess its performance. Subsequently, the calibrated model variables were further tested on airborne data from Cullingral in order to study their robustness and to verify the parameterization derived from the Merriwa Park study site. The assumption that the remaining vegetation values as proposed by [15] for i) the vegetation parameter b and ii) the single scattering albedo ω were representative was justified based on: i) a site-specific calibration across the available observation dates that showed no significant variations from b=0.08 and ω =0 and ii) the fact that the parameterization resulted from an extensive literature review by [15]. Further analysis of the three parameterizations included the inversion of the L-MEB model to solve an optimization problem for the retrieval of soil moisture given *a priori* ground truth information. The algorithm was based on a minimized cost function that calculated the quadratic difference between the measured and simulated brightness temperatures.

V. Results and Discussion

The comparison of the L-MEB predicted brightness temperature response with the airborne multi-angle observations from Merriwa Park and Cullingral for incidence angles ranging from 0-50° showed significant discrepancies depending on the model parameterization chosen (Fig. 2). Using the default L-MEB parameterization, the forward model consistently underestimated the multi-angle observations at H-polarization, whereas at V-polarization (especially for large incidence angles and wet soil conditions) the simulated brightness temperatures were much higher than those observed. Furthermore, the exhibited angular trends of the dual-polarized observations were only partially captured by the simulation results. Hence, differences of up to ~40 K in brightness temperatures were observed, particularly within the range of low angles. While this difference decreased for the vertical polarized curve with larger incidence angles, the simulated horizontal brightness temperatures were always lower than the measured data. Note, that for wet conditions at Merriwa Park during the first two observation days, the simulated horizontally polarized curve is relatively flat due to the high vegetation water content and the corresponding large value for the optical depth. The explanation behind this trend is that both the attenuation of the soil emission and the emission by the wheat canopy itself increased, causing the effective composite brightness temperature of both media to be closer to the effective temperature of the vegetation. So with larger incidence angles, the attenuation of the vegetation increased with respect to the 1/cos(θ) relationship as shown in equation (3). Setting a default value of 1 for tt_h further assumes that there are no significant angular dependencies across the observed wheat canopy at H-polarization. The comparison of the predicted and observed brightness temperatures across the four observation days at Merriwa Park produced a root mean square error (rmse) ranging from 38 K to 26 K for wet and dry conditions, respectively (Fig. 3), when using the default parameters.

The overall model performance was improved by introducing the soil moisture dependent roughness value H_r (second model parameterization) from the site-specific calibration presented by [26]. Consequently, an upward translation of the modelled brightness temperature curves was achieved resulting in a closer agreement with the actual observations. The corresponding root mean square errors ranged between 9.6 K (wet) to 2.9 K (dry), and were thus significantly reduced compared to the default model parameterization output. However, the simulated angular behaviour was still unable to capture the observed brightness temperature trend exhibited at large angles (> 25°), which was especially dominant for moist conditions at Merriwa Park at the start of the campaign. Moreover, for relatively low moisture contents (< 0.1 m^3m^{-3}) the curve shift forced by the moisture adjusted roughness value towards higher brightness temperatures was too strong. Hence, the predicted emissions tended to overestimate the brightness temperature measurements especially for dry conditions. A site-specific calibration of H_r based on the multi-angle observations available for Merriwa Park (not shown in this paper) confirmed a non-linear relationship between soil moisture and surface roughness. Specifically, the calibration showed i) a positive correlation between surface roughness and soil moisture for dry conditions resulting in small H_r values for dry soil, and ii) a negative trend for soil moisture values of ~0.20 m^3m^{-3} or higher by decreasing the roughness effect with increasing moisture content. These findings also agreed with the results published by [31] who investigated the impact of soil moisture on surface roughness using single-angle NAFE'05 data. In that study the decrease of the roughness effect for low soil moisture was associated with a reduced dielectric heterogeneity at micro-scale during the drying process of the clay loam soils that dominate the study area. That is, the micro-scale variability and thus the dielectric roughness would peak at intermediate soil moisture content and decrease in very wet or very dry conditions. Hence, applying a reduced roughness parameter from a non-linear function for dry conditions would ultimately produce better results when comparing the forward simulations and the airborne measurements. The current SMOS Level 2 soil moisture retrieval algorithms [23] include the sensitivity of surface roughness on soil moisture in terms of a simple linear function such as that applied in this study. The roughness estimation, however, is confined by the field capacity as an upper limit and a transition moisture point as the lower limit, with both parameters being a function of the soil texture (sand/clay content). Above and below these two points the roughness value is a constant, and the minimum

H_r value is expressed by $H_rMIN=(2k\sigma)^2$ [32], with k being the wave number and σ defined as the surface root mean square height. Note, that i) the corresponding minimum and maximum H_r values are dependent on the actual land cover type observed and ii) the maximum H_rMAX parameter is retrieved from the individual SMOS scene.

The L-MEB parameterization of the third model included i) the moisture dependent roughness factor H_r tested in the second model approach and ii) specifically calibrated vegetation structure parameters tt_h and tt_v that account for the angular dependency of the vegetation attenuation. The corresponding forward model results showed the overall best agreement with the airborne data (rmse=2.5-5.3 K) and the trend of the predicted dual-polarization curves captured that of the measured data for both moist and dry soil moisture conditions. Compared to the default parameterization and the high tt_v value of 8 obtained for the vertically dominated wheat canopy [15], the vegetation structure parameters calibrated and tested in this study were significantly lower and closer to unity (~1). Though it should be noted, that an individual calibration of the tt_P parameters for each single day suggested a value of tt_v = 3 in one case, but overall only minor variations across the different dates were observed. Consequently, the calibrated vegetation structure parameters from the 9th of November 2005 were validated on different moisture conditions and locations (Cullingral), confirming the good results obtained using this particular parameterization. Further analysis showed that using the individually estimated tt_P values for each observation day, instead of the values calibrated from the 9 November 2005, improved the model rmse performance by 0.1 K at most. Moreover, the results demonstrated that the adjustment of both angular correction parameters had a more significant impact on the predicted brightness temperatures, when the ground measured vegetation water content was high (>1.9 kg/m^2) and thus, the attenuation effects of the canopy and its own contribution to the composite brightness temperature increased as well. Consequently, both structure parameters play a major role especially for large incidence angles (> 30°) where the path length of the emitted energy through the vegetation layer is longer.

The soil moisture retrieval based on an iterative least-squared algorithm resulted in a range of soil moisture values depending on the model parameterizations chosen (Fig. 4). The default parameterization generally produced too low soil moisture values with a maximum difference of ~0.3 m^3m^{-3}, if compared against the measured soil moisture. The overall best result with the retrieved soil moisture being close (≤0.04 m^3m^{-3}) to the observed moisture conditions was achieved using the optimized set of parameters, which included the soil moisture dependent roughness value H_r and the calibrated vegetation structure values tt_P (third model approach).

VI. Conclusion

This paper has presented simulations of brightness temperatures at a range of incidence angles and the subsequent comparison with multi-incidence angle airborne observations over two wheat canopy test sites in eastern Australia. The forward model used in this research was the L-band Microwave Emission of the Biosphere (L-MEB) model which is one of the core elements of the SMOS soil moisture retrieval algorithm. Apart from the default model parameterization proposed by [15], two additional parameterizations were studied, including modifications of the surface roughness and vegetation structure characterization. The performance of the individual model approach was not only assessed based on changing moisture conditions, but also for different locations in order to test its robustness. The agreement of the predicted and the measured brightness temperature data from different the forward model parameterizations varied significantly; with the observed discrepancy being much larger for wet conditions than for dry soil moisture values. However, compared to the results using the default model parameterization, a stepwise improvement was achieved by firstly introducing a soil moisture dependent roughness factor and secondly by optimizing the vegetation structure parameters. Consequently, the dual-polarized brightness temperature predictions were improved by minimizing the rmse from 38.1 K to 2.3 K for wet soil conditions (~0.45 m^3m^{-3}) and from 26.5 K to 5.3 K for dry soils (~0.13 m^3m^{-3}).

This study proves that neglecting the sensitivity of the surface roughness parameter H_r on soil moisture leads to a significant underestimation of the soil emission at L-band, which would consequently affect the overall soil moisture retrieval accuracy. Furthermore, it was shown that the transmissivity of a dominantly vertical canopy structure and the angular dependency of the optical depth should not be neglected for vegetation water contents of >1.9 kg/m^2 and wet soil conditions (> 0.4 m^3m^{-3}), otherwise the error introduced into the retrieved soil moisture product for the given data set could be up to 0.3 m^3m^{-3}. Though it should be noted that considering the spatial resolution of SMOS observations and a footprint size of approximately ~42 km, which captures a mixture of land cover types, the angular effect is likely to be minor for SMOS products. However, this issue needs to be investigated in future research to understand the impact of the angular vegetation structure effects on the soil moisture retrieval at satellite scale. Based on the demonstrated results, the effect of dominantly vertically structured canopies should be assessed by comparing the single-angle and multi-angle soil moisture retrieval performance using both passive microwave data from airborne observations and SMOS.

VII. Acknowledgment

The authors would like to thank the NAFE'05 team for collecting and providing the data set used in this study. This work was supported by the Australian Research Council (DP0879212) within the framework of the Moisture Map project.

REFERENCES

[1] T. J. Schmugge, P. E. O'Neill, and J. R. Wang, "Passive microwave soil moisture research," *IEEE Trans. Geosci. Remote Sens.,* vol. GE-24, no. 1, pp. 12-22, 1986.

[2] J. C. Calvet, J. P. Wigneron, A. Chanzy, and D. Haboudane, "Retrieval of surface parameters from microwave radiometry over open canopies at high frequencies," *Remote Sens. Environ.,* vol. 53, pp. 46-60, 1995.

[3] T. J. Jackson, J. Schmugge, and E. T. Engman, "Remote sensing applications to hydrology: Soil moisture," *Hydrol. Sci. J.,* vol. 41, no. 4, pp. 517-530, 1996.

[4] E. G. Njoku and D. Entekhabi, "Passive microwave remote sensing of soil moisture," *J. Hydrol.,* vol. 184, no. 1-2, pp. 101-129, 1996.

[5] C. Pathe, W. Wagner, D. Sabel, M. Doubkova, and J. B. Basara, "Using ENVISAT ASAR Global Mode Data for Surface Soil Moisture Retrieval Over Oklahoma, USA," *IEEE Trans. Geosci. Remote Sens.,* vol. 47, pp. 468-480, 2009.

[6] C. Rüdiger, J.-C. Calvet, C. Gruhier, T. R. H. Holmes, R. A. M. de Jeu, and W. Wagner, "An Intercomparison of ERS-Scat and AMSR-E Soil Moisture Observations with Model Simulations over France," *J. Hydrometeorol.,* vol. 10, pp. 431-447, 2009.

[7] J. Wigneron, J. Calvet, T. Pellarin, A. Van de Griend, M. Berger, and P. Ferrazzoli, "Retrieving near-surface soil moisture from microwave radiometric observations: current status and future plans," *Remote Sens. Environ.,* vol. 85, no. 4, pp. 489-506, 2003.

[8] J. Leese, T. Jackson, A. Pitman, and P. Dirmeyer, "GEWEX/BAHC International workshop on soil moisture monitoring, analysis, and prediction for hydrometeorological and hydroclimatological applications," *Bulletin of the American Meteorological Society,* vol. 82, pp. 1423-1430, 2001.

[9] Y. Kerr, P. Waldteufel, J. P. Wigneron, J. M. Martinuzzi, J. Font and M. Berger, "Soil moisture retrieval from space: The Soil Moisture and Ocean Salinity (SMOS) mission," *IEEE Trans. Geosci. Remote Sens.* vol. 39, no. 8: pp. 1729-1735, Aug. 2001.

[10]Y. Kerr, P. Waldteufel, J. Wigneron, S. Delwart, F. Cabot, J. Boutin, M. Escorihuela, J. Font, N. Reul, and C. Gruhier, "The SMOS Mission: New Tool for Monitoring Key Elements of the Global Water Cycle," *Proceedings of the IEEE,* vol. 98, pp. 666-687, 2010.

[11]M. Pardé, J. P. Wigneron, A. Chanzy, P. Waldteufel, Y. Kerr, and S. Huet, "Retrieving surface soil moisture over a wheat field: comparison of different methods," *Remote Sens. Environ.*, vol. 87, pp. 334-344, 2003.

[12]M. J. Sandells, I. J. Davenport, and R. J. Gurney, "Passive L-band microwave soil moisture retrieval error arising from topography in otherwise uniform scenes," *Adv. Water Resour.*, vol. 31, pp. 1433-1443, 2008.

[13]J. Wigneron, M. Parde, P. Waldteufel, A. Chanzy, Y. Kerr, S. Schmidl, and N. Skou, "Characterizing the dependence of vegetation model parameters on crop structure, incidence angle, and polarization at L-band," *IEEE Trans. Geosci. Remote Sens.,* vol. 42, pp. 416-425, Feb. 2004.

[14]J. Wigneron, P. Waldteufel, A. Chanzy, J. Calvet, and Y. Kerr, "Two-dimensional microwave interferometer retrieval capabilities over land surfaces(SMOS Mission)," *Remote Sens. Environ.,* vol. 73, pp. 270-282, 2000.

[15]J. Wigneron, Y. Kerr, P. Waldteufel, K. Saleh, M. Escorihuela, P. Richaume, P. Ferrazzoli, P. de Rosnay, R. Gurney, and J. Calvet, "L-band Microwave Emission of the Biosphere (L-MEB) Model: Description and calibration against experimental data sets over crop fields," *Remote Sens. Environ.,* vol. 107, pp. 639-655, Apr. 2007.

[16]I. Davenport, J. Fernandez-Galvez, and R. Gurney, "A sensitivity analysis of soil moisture retrieval from the tau-omega microwave emission model," *IEEE Trans. Geosci. Remote Sens.,* vol. 43, pp. 1304-1316, 2005.

[17]P. de Rosnay, J. Calvet, Y. Kerr, J. Wigneron, F. Lemaître, M. Escorihuela, J. Sabater, K. Saleh, J. Barrié, and G. Bouhours, "SMOSREX: A long term field campaign experiment for soil moisture and land surface processes remote sensing," *Remote Sens. Environ.,* vol. 102, pp. 377-389, 2006.

[18]A. Cano, K. Saleh, J.-P. Wigneron, C. Antolín, J. E. Balling, Y. H. Kerr, A. Kruszewski, C. Millán-Scheiding, S. S. Søbjærg, N. Skou, and E. López-Baeza, "The SMOS Mediterranean Ecosystem L-Band characterisation EXperiment (MELBEX-I) over natural shrubs," *Remote Sens. Environ.,* vol. 114, pp. 844-853, 2010.

[19]K. Saleh, J. Wigneron, J. Calvet, E. Lopez-Baeza, P. Ferrazzoli, M. Berger, P. Wursteisen, L. Simmonds, and J. Miller, "The EuroSTARRS airborne campaign in support of the SMOS mission: first results over land surfaces," *J. Remote Sens.,* vol. 25, pp. 177-194, 2004.

[20]R. Panciera, J. P. Walker, J. D. Kalma, E. J. Kim, J. M. Hacker, O. Merlin, M. Berger, and N. Skou, "The NAFE'05/CoSMOS Data Set: Toward SMOS Soil Moisture Retrieval, Downscaling, and Assimilation," *IEEE Trans. Geosci. Remote Sens.,* vol. 46, pp. 736-745, Mar. 2008.

[21]C. Rüdiger, G. Hancock, H. M. Hemakumara, B. Jacobs, J. D. Kalma, C. Martinez, M. Thyer, J. P. Walker, T. Wells, and G. R. Willgoose, "Goulburn River experimental catchment data set," *Water Resour. Res.,* vol. 43, p. W10403, 2007.

[22]O. Merlin, J. Walker, R. Panciera, R. Young, J. Kalma, and E. Kim, "Soil moisture measurement in heterogeneous terrain," *MODelling and SIMulation Society of Australia and New Zealand. New Zealand,* 2007.

[23]Y. Kerr, P. Waldteufel, P. Richaume, P. Ferrazzoli, and J. Wigneron, "SMOS level 2 Processor for Soil Moisture Algorithm Theoretical Based Document (ATBD)," CESBIO, Toulouse, SO-TN-ESL-SM-GS-0001, v3.a., Oct. 15, 2008.

[24]T. J. Jackson and T. J. Schmugge, "Vegetation effects on the microwave emission of soils," *Remote Sens. Environ.,* vol. 36, pp. 203-212, 1991.

[25]J. Wigneron, A. Chanzy, J. Calvet, and N. Bruguier, "A simple algorithm to retrieve soil moisture and vegetation biomass using passive microwave measurements over crop fields," *Remote Sens. Environ.,* vol. 51, pp. 331-341, Aug. 1995.

[26]R. Panciera, J. Walker, J. Kalma, E. Kim, K. Saleh, and J. Wigneron, "Evaluation of the SMOS L-MEB passive microwave soil moisture retrieval algorithm," *Remote Sens. Environ.,* vol. 113, pp. 435-444, Feb. 2009.

[27]J. Wigneron, L. Laguerre, and Y. Kerr, "A simple parameterization of the L-band microwave emission from rough agricultural soils," *IEEE Trans. Geosci. Remote Sens.,* vol. 39, pp. 1697-1707, Aug. 2001.

[28]T. Mo and T. Schmugge, "A parameterization of the effect of surface roughness on microwave emission," *IEEE Trans. Geosci. Remote Sens.,* vol. 25, pp. 47-54, Jan. 1987.

[29]K. Saleh, Y. H. Kerr, P. Richaume, M. J. Escorihuela, R. Panciera, S. Delwart, G. Boulet, P. Maisongrande, J. P. Walker, and P. Wursteisen, "Soil moisture retrievals at L-band using a two-step inversion approach (COSMOS/NAFE'05 Experiment)," *Remote Sens. Environ.,* vol. 113, pp. 1304-1312 2009.

[30]M. Escorihuela, Y. Kerr, P. de Rosnay, J. Wigneron, J. Calvet, and F. Lemaitre, "A Simple Model of the Bare Soil Microwave Emission at L-Band," *IEEE Trans. Geosci. Remote Sens.*, vol. 45, pp. 1978-1987, 2007.

[31]R. Panciera, J. Walker, and O. Merlin, "Improved Understanding of Soil Surface Roughness Parameterization for L-Band Passive Microwave Soil Moisture Retrieval," *IEEE Trans. Geosci. Remote Sens. Lett.,* vol. 6, pp. 625-629, Oct. 2009.

[32]B. Choudhury, T. J. Schmugge, A. Chang, and R. Newton, "Effect of surface roughness on the microwave emission from soils," *J. Geophysical Res.,* vol. 84, pp. 5699-5706, 1979

511

TABLES

TABLE I: Characteristics of selected NAFE'05 focus farms with multi-incidence angle observations

TABLE II: Parameterization of the three forward models studied

FIGURES

Fig. 1. Locations of NAFE'05 Focus farms, multi-angle flight lines, soil moisture measurements and monitoring stations in the Goulburn River catchment, New South Wales, Australia.

Fig. 2. Dual-polarized brightness temperature estimates plotted against incidence angle and compared to multi-angle PLMR observations over wheat canopy available for Merriwa Park and Cullingral. The forward simulations were based on three different model parameterization (default, Hr-cal, optimized) as given in Table II. Note, that only the data from 9 Nov 2005 at Merriwa Park were used for model calibration (optimized model), whereas the remaining datasets were used for validation purpose.

Fig. 3. Scatterplot of the L-MEB model simulations in comparison with independent ground data from Merriwa Park at different observation dates using the default model parameterization (dots) [15], the site-specific roughness parameterization (crosses) [26] and the optimized model parameterization (circles). The root mean square errors [K] are given for all model approaches.

Fig. 4. Scatterplot showing the retrieved against the measured soil moisture values at the Merriwa Park focus farm for the four available observation days. The inverse application of the L-MEB model was made for all three model parameterizations discussed in Section IV.

TABLE I
CHARACTERISTICS OF SELECTED NAFE'05 FOCUS FARMS WITH MULTI-INCIDENCE ANGLE OBSERVATIONS

SITE	OBSERVATIONS DAYS	LAND COVER	TOPOGRAPHY	SOIL TYPE	SAND CONTENT [%]	CLAY CONTENT [%]	VEGETATION WATER CONTENT[a] MIN-MAX [kg/m²]	SOIL MOISTURE[a] MIN-MAX [m³/m³]
Merriwa Park	4	Native grass + agriculture (wheat)	Gently sloping	Silt clay loam	21	30	0.70 - 3.00	0.10 – 0.50
Cullingral	1	Native grass + agriculture (wheat/barley)	Flat	Silty loam	36	26	0.14 – 0.47	0.03 – 0.09

[a]across area with wheat cover

TABLE II
PARAMETERIZATION OF THE THREE FORWARD MODELS STUDIED

MODEL	ROUGHNESS H_r	N_{rh}	N_{rv}	VEGETATION tt_h	tt_v	ω_h	ω_v	COMMENT
Default	0.1	0	0	1	8	0	0	Parameterization proposed by [15]
Hr-cal	1.5-1.6·SM[a]* 1.6-1.0·SM[a]**	0	0	1	8	0	0	Soil moisture dependent H_r component [26]
Optimized	1.5-1.6·SM[a]* 1.6-1.0·SM[a]**	0	0	0.2	1.4	0	0	Soil moisture dependent H_r [26] and optimized vegetation structure values calibrated from multi-incidence angle data from Merriwa Park 09/11/2005

[a]SM: Soil Moisture; *Roughness function for Merriwa Park; **Roughness function for Cullingral

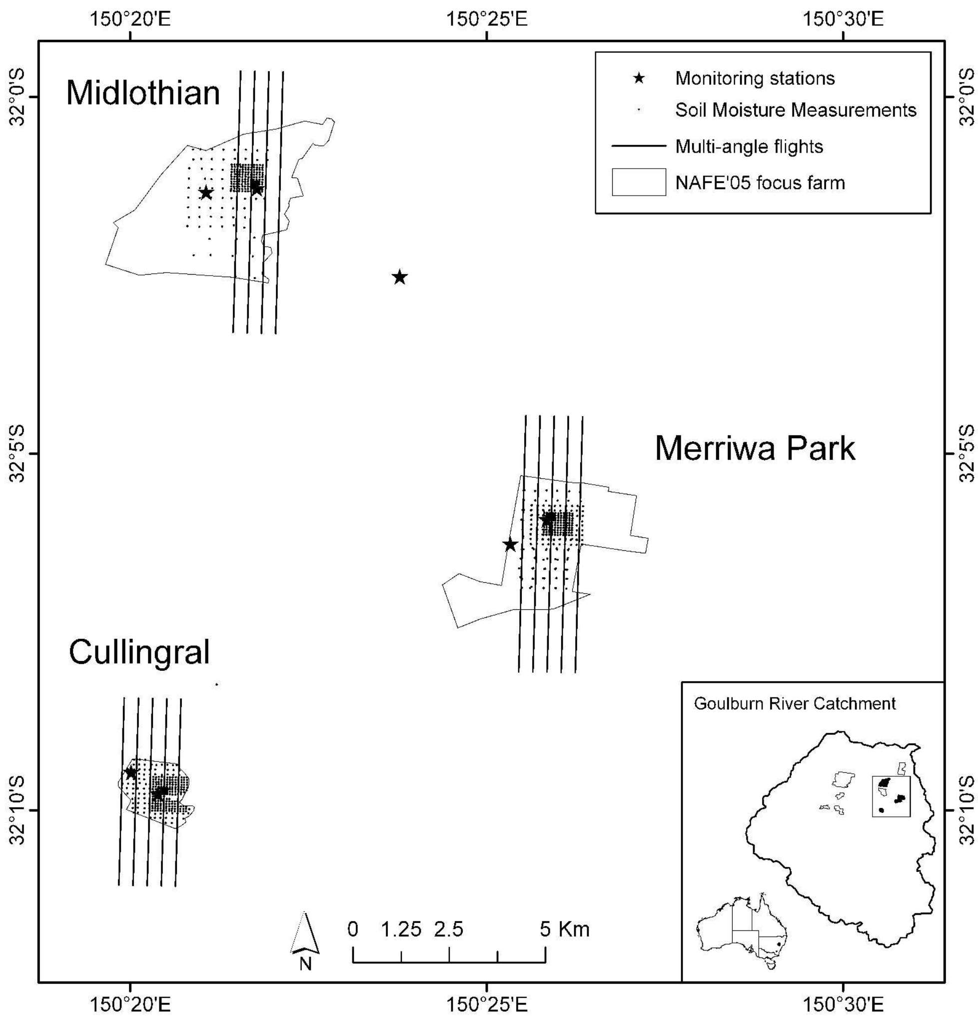

Fig. 1. Locations of NAFE'05 Focus farms, multi-angle flight lines, soil moisture measurements and monitoring stations in the Goulburn River catchment, New South Wales, Australia.
206x212mm (600 x 600 DPI)

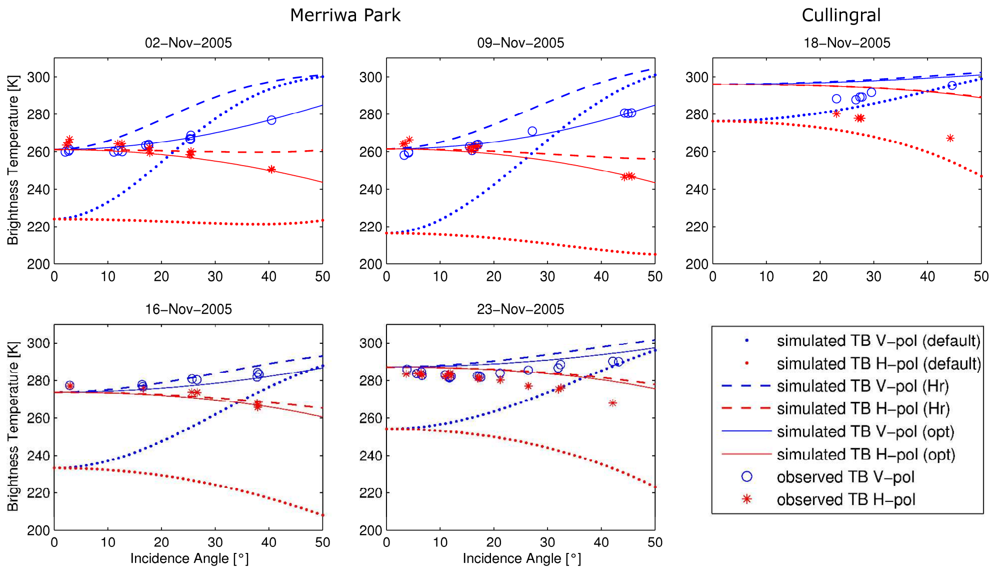

Fig. 2. Dual-polarized brightness temperature estimates plotted against incidence angle and compared to multi-angle PLMR observations over wheat canopy available for Merriwa Park and Cullingral. The forward simulations were based on three different model parameterization (default, Hr-cal, optimized) as given in Table II. Note, that only the data from 9 Nov 2005 at Merriwa Park were used for model calibration (optimized model), whereas the remaining datasets were used for validation purpose.
253x145mm (600 x 600 DPI)

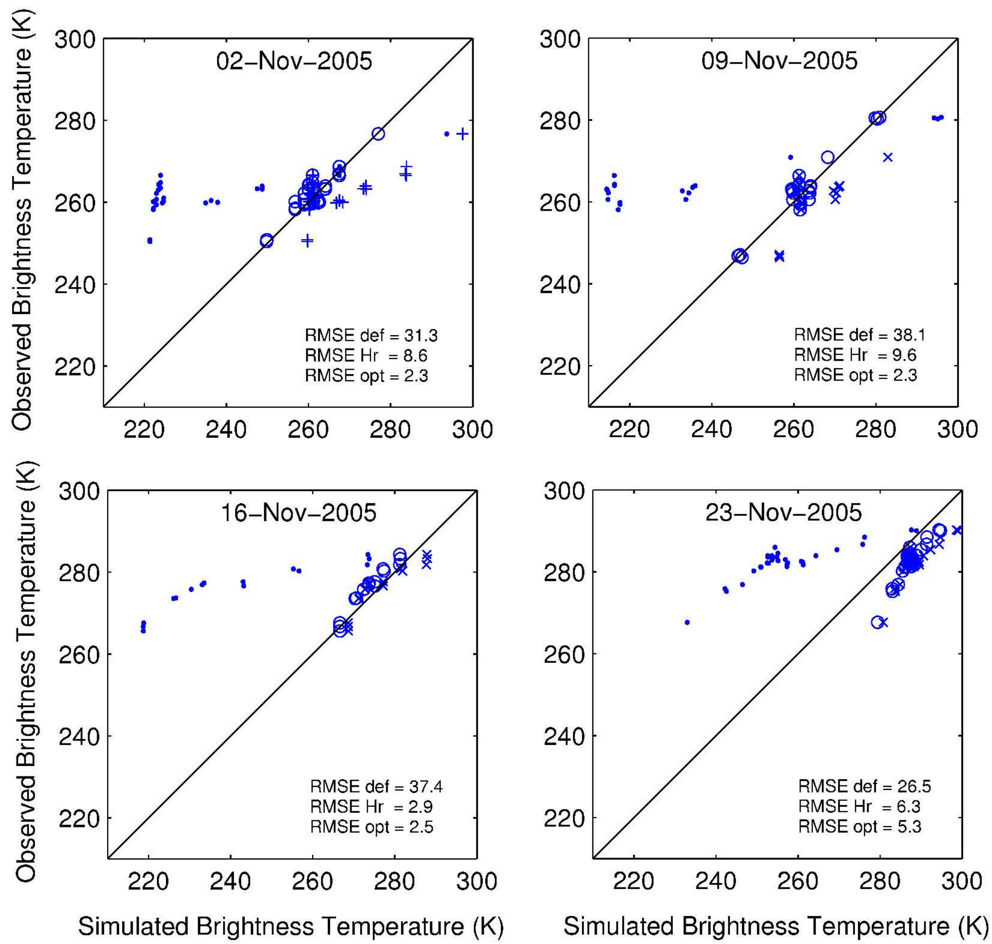

Fig. 3. Scatterplot of the L-MEB model simulations in comparison with independent ground data from Merriwa Park at different observation dates using the default model parameterization (dots) [15], the site-specific roughness parameterization (crosses) [26] and the optimized model parameterization (circles). The root mean square errors [K] are given for all model approaches.
141x134mm (600 x 600 DPI)

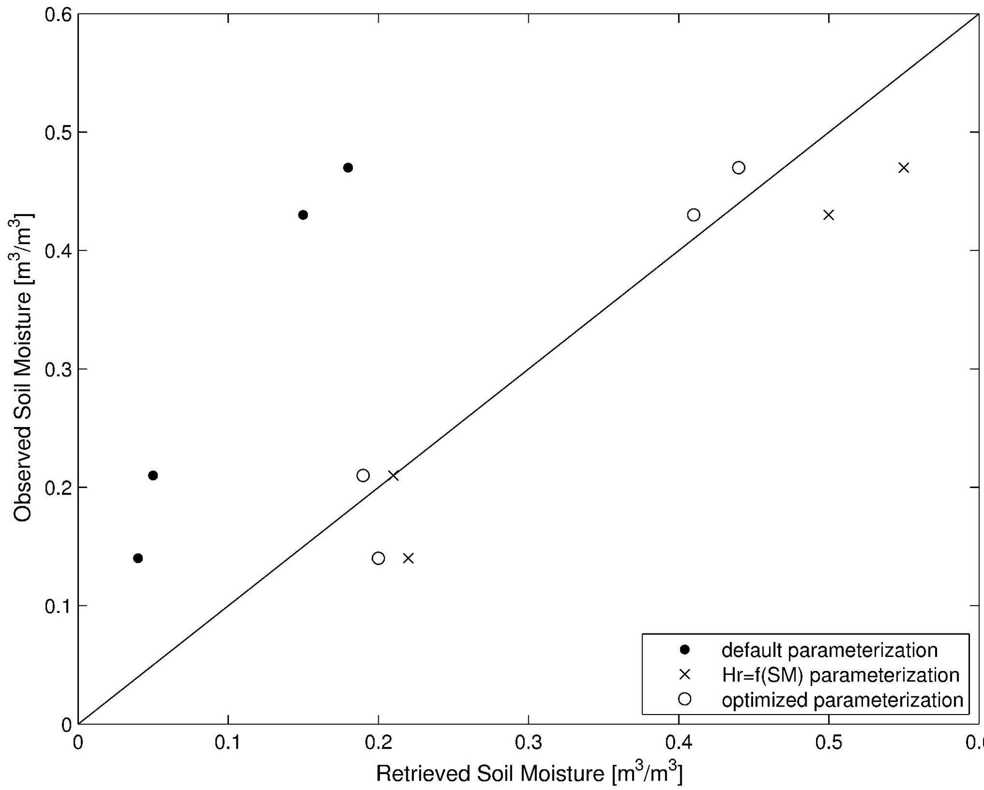

Fig. 4. Scatterplot showing the retrieved against the measured soil moisture values at the Merriwa Park focus farm for the four available observation days. The inverse application of the L-MEB model was made for all three model parameterizations discussed in Section IV.
174x140mm (600 x 600 DPI)